Analysis of $B \to K_J^*(\to K\pi)\mu^+\mu^-$ in the higher kaon resonance region

Cai-Dian Lü [a] and Wei Wang [b] *

[a] Institute of High Energy Physics, P.O. Box 918(4), Beijing 100049, People's Republic of China
[b] Deutsches Elektronen-Synchrotron DESY, Hamburg 22607, Germany

We study the resonant contributions in the process of $\overline{B}^0 \to K^-\pi^+\mu^+\mu^-$ with the $K^-\pi^+$ invariant mass square $m_{K\pi}^2 \in [1,5]\mathrm{GeV}^2$. Width effects of the involved strange mesons, $K^*(1410), K_0^*(1430), K_2^*(1430), K^*(1680), K_3^*(1780)$ and $K_4^*(2045)$, are incorporated. In terms of helicity amplitudes, we derive a compact form for the full angular distributions, through which the branching ratios, forward-backward asymmetries and polarizations are attained. We propose that the uncertainties in the $B \to K_J^*$ form factors can be pinned down by the measurements of a set of SU(3)-related processes. Using results from the large energy limit, we derive the dependence of branching fractions on the $m_{K\pi}$, and find that the K_2^* resonance has a clear signature, in particular, in the transverse polarizations.

PACS numbers: 13.20.He; 12.39.St 14.40.Be;

I. INTRODUCTION

It is anticipated that the LHC is able to answer some of the fundamental questions in particle physics. One of great interests is in dertermining whether the new degrees of freedom are relevant for the phenomena at the TeV scale. On the one hand, many new particles have signatures different from the standard model (SM) particles, and measurements of their production and decays at the LHC may provide definitive evidence on their existence. On the other hand, low energy processes may also be influenced by them. Rare B decays, with tiny decay probabilities in the SM, are highly sensitive to the new degrees of freedom and thus can be exploited as indirect searches of these unknown effects. In particular, $b \to sl^+l^-$ especially $B \to K^*(\to K\pi)l^+l^-$ provide a wealth of information on the weak interactions, in terms of a number of observables ranging from the decay probabilities, forward-backward asymmetries (FBAs), polarizations to a full angular analysis. The small branching fraction, of order 10^{-6} for $B \to K^*l^+l^-$, is compensated by the high luminosity at the B factories and hadron colliders [1–3]. It is anticipated that the measurements by the LHCb detector will allow to probe the short-distance physics at an unprecedented level and will provide good sensitivity to discriminate between the SM and different models of new physics. For instance, results by the LHCb based on the data with the integrated luminosity $0.3fb^{-1}$ [4] are in good agreement with the theory predictions [5], which has placed a stringent constraint on new physics (NP) models.

In our previous work [6], we have explored the $B \to K_2^*l^+l^-$ decay mode in the SM and two specific NP scenarios using the $B \to K_2^*$ form factors calculated in Ref. [7]. We provided a comprehensive analysis of the branching ratio, FBAs, transversity amplitudes, and full angular distributions. It is pointed out that the $B \to K_2^*l^+l^-$ decay has several advantages in different aspects and is complementary to the commonly-studied mode $B \to K^*l^+l^-$. The process $B \to K_2^*l^+l^-$ has also received considerable attention in the SM and several variants of it in Refs. [8–13]. On

---

* Email: wei.wang@desy.de

TABLE I: Wilson coefficients $C_i(m_b)$ in the leading logarithmic approximation, with $m_W = 80.4 \text{GeV}$, $\mu = m_{b,\text{pole}}$ [15].

C_1	C_2	C_3	C_4	C_5	C_6	C_7^{eff}	C_9	C_{10}
1.107	-0.248	-0.011	-0.026	-0.007	-0.031	-0.313	4.344	-4.669

the experimental side, however, its usefulness is challenged by the "pollution" from several other strange resonances in this mass region namely $K^*(1410), K_0^*(1430), K^*(1680), K_3^*(1780)$ and $K_4^*(2045)$ [14]. The different contributions can be separated by a partial wave analysis when a large amount of data is available, but it is necessary to explore the interference effects in physical quantities, such as the branching ratios to have a benchmark for the possible measurement in the first running of LHC. The aim of the present work is to achieve this goal. To do so, we will study the $B \to K_J^* l^+ l^- \to K\pi l^+ l^-$ with the invariant mass square $m_{K\pi}$ ranging from 1 to 5 GeV^2. Using the helicity amplitudes technique we will derive a compact form for the angular distributions and a number of other quantities. To reduce the uncertainties in $B \to K_J^*$ transition form factors, we will propose to measure a set of useful but SU(3)-related channels. In terms of the results derived from the large energy symmetry, we will show the differential distributions and their dependence on $m_{K\pi}^2$. We further point out that for $m_{K\pi}^2 \simeq 2\text{GeV}^2$, the K_2^* dominates especially in the transverse polarization while at $m_{K\pi}^2 \simeq 3\text{GeV}^2$, the $B \to K^*(1680)$ contribution is the largest.

The rest of the paper is organized as follows. In Sec. II, we give the theoretical framework including the effective Hamiltonian and the hadronic form factors. Sec. III is devoted to the derivation of the differential decay distributions and the integrated quantities. Sec. IV is devoted to the numerical predictions in the SM. We conclude in the last section. The appendix contains our derivation of the angular distributions.

II. THEORETICAL FRAMEWORK

The decay amplitude for $B \to K_J^*(\to K\pi)l^+l^-$ consists of two separate parts: the short distance physics and the long-distance physics. The former arises from the degrees of freedom higher than m_b, and thus can be computed by perturbation theory. The low-energy effect is usually parameterized in terms of heavy-to-light form factors.

The $b \to sl^+l^-$ effective Hamiltonian

$$\mathcal{H}_{\text{eff}} = -\frac{G_F}{\sqrt{2}} V_{tb} V_{ts}^* \sum_{i=1}^{10} C_i(\mu) O_i(\mu)$$

involves the four-quark and the magnetic penguin operators O_i and their explicit forms can be found in Ref. [15]. Here $C_i(\mu)$ are the Wilson coefficients for these local operators O_i, and we use the leading logarithmic values [15], which are listed in Table I, G_F is the Fermi constant, $V_{tb} = 0.999176$ and $V_{ts} = -0.03972$ [14] are the CKM matrix elements. The double Cabibbo suppressed terms, proportional to $V_{ub}V_{us}^*$, have been omitted. $m_b = 4.67^{+0.18}_{-0.06}\text{GeV}$ and $m_s = 0.101^{+0.029}_{-0.021}\text{GeV}$ are the b and s quark masses [14].

With the neglect of QCD corrections, only the operators $O_{7\gamma}, O_9$ and O_{10} contribute to the decay amplitudes

$$
\begin{aligned}
i\mathcal{M}(b \to sl^+l^-) &= \frac{iG_F}{\sqrt{2}} \frac{\alpha_{\text{em}}}{\pi} V_{tb}V_{ts}^* \times \left(\frac{C_9 + C_{10}}{4}[\bar{s}b]_{V-A}[\bar{l}l]_{V+A} + \frac{C_9 - C_{10}}{4}[\bar{s}b]_{V-A}[\bar{l}l]_{V-A} \right.\\
&\left. + C_{7L}m_b[\bar{s}i\sigma_{\mu\nu}(1+\gamma_5)b]\frac{q^\mu}{q^2} \times [\bar{l}\gamma^\nu l] + C_{7R}m_b[\bar{s}i\sigma_{\mu\nu}(1-\gamma_5)b]\frac{q^\mu}{q^2} \times [\bar{l}\gamma^\nu l] \right),
\end{aligned}
\tag{1}
$$

TABLE II: Properties of the resonances K_J^*. The isospin symmetry relation $\mathcal{B}(K_J^* \to K^-\pi^+) = 2/3\mathcal{B}(K_J^* \to K\pi)$ will be used.

K_J^*	J^P	$n^{2S+1}L_J$	m (MeV)	Γ (MeV)	$\mathcal{B}(K_J^* \to K\pi)(\%)$	α_L	β_T
$K^*(1410)$	1^-	2^3S_1?	1414 ± 15	232 ± 21	6.6 ± 1.3	1	1
$K_0^*(1430)$	0^+	$1^3P_0, 2^3P_0$?	1425 ± 50	270 ± 80	93 ± 10	1	$-$
$K_2^*(1430)$	2^+	$^3P_2$	1432.4 ± 1.3	109 ± 5	49.9 ± 1.2	$\sqrt{\frac{2}{3}}$	$\sqrt{\frac{1}{2}}$
$K^*(1680)$	1^-	1^3D_1	1717 ± 27	322 ± 110	38.7 ± 2.5	1	1
$K_3^*(1780)$	3^-	1^3D_3	1776 ± 7	159 ± 21	18.8 ± 1.0	$\sqrt{\frac{2}{5}}$	$\sqrt{\frac{4}{15}}$
$K_4^*(2045)$	4^+	1^3F_4	2045 ± 9	198 ± 30	9.9 ± 1.2	$\sqrt{\frac{8}{35}}$	$\sqrt{\frac{1}{7}}$

TABLE III: $B \to K_J^*$ form factors taken from Ref. [10].

K_J^*	$\xi_{\parallel}$	$\xi_{\perp}$
$K^*(1410)$	0.22 ± 0.03	0.28 ± 0.04
$K_0^*(1430)$	0.22 ± 0.03	$-$
$K_2^*(1430)$	0.22 ± 0.03	0.28 ± 0.04
$K^*(1680)$	0.18 ± 0.03	0.24 ± 0.05
$K_3^*(1780)$	0.16 ± 0.03	0.23 ± 0.05
$K_4^*(2045)$	0.13 ± 0.03	0.19 ± 0.05

where $C_{7L} = C_7$ and $C_{7R} = \frac{m_s}{m_b}C_{7L}$. On the other hand, the operators $O_1 - O_6$ also contribute starting from the one loop diagrams. The factorizable loop terms can be incorporated into the Wilson coefficients C_7 and C_9, and thus it is convenient to define the Wilson coefficients combinations $C_7^{\rm eff}$ and $C_9^{\rm eff}$ [16]

$$
\begin{aligned}
C_7^{\rm eff} &= C_7 - C_5/3 - C_6, \\
C_9^{\rm eff}(q^2) &= C_9(\mu) + h(\hat{m}_c, \hat{s})C_0 - \frac{1}{2}h(1, \hat{s})(4C_3 + 4C_4 + 3C_5 + C_6) \\
&\quad - \frac{1}{2}h(0, \hat{s})(C_3 + 3C_4) + \frac{2}{9}(3C_3 + C_4 + 3C_5 + C_6),
\end{aligned}
\tag{2}
$$

with $\hat{s} = q^2/m_b^2$, $C_0 = C_1 + 3C_2 + 3C_3 + C_4 + 3C_5 + C_6$, and $\hat{m}_c = m_c/m_b$. The auxiliary functions used above are

$$
\begin{aligned}
h(z, \hat{s}) &= -\frac{8}{9}\ln\frac{m_b}{\mu} - \frac{8}{9}\ln z + \frac{8}{27} + \frac{4}{9}x - \frac{2}{9}(2+x)|1-x|^{1/2}
\begin{cases}
\ln\left|\frac{\sqrt{1-x}+1}{\sqrt{1-x}-1}\right| - i\pi & \text{for } x \equiv \frac{4z^2}{\hat{s}} < 1 \\
2\arctan\frac{1}{\sqrt{x-1}} & \text{for } x \equiv \frac{4z^2}{\hat{s}} > 1
\end{cases}, \\
h(0, \hat{s}) &= -\frac{8}{9}\ln\frac{m_b}{\mu} - \frac{4}{9}\ln\hat{s} + \frac{8}{27} + \frac{4}{9}i\pi.
\end{aligned}
\tag{3}
$$

In the following, we shall also drop the superscripts for $C_9^{\rm eff}$ and $C_7^{\rm eff}$ for brevity.

The $B \to K_0^*(1430)$ transition form factors are defined by

$$
\begin{aligned}
\langle K_0^*(P_2)|\bar{s}\gamma_\mu\gamma_5 b|\overline{B}(P_B)\rangle &= -i\left\{\left[P_\mu - \frac{m_B^2 - m_{K_0^*}^2}{q^2}q_\mu\right]F_1(q^2) + \frac{m_B^2 - m_{K_0^*}^2}{q^2}q_\mu F_0(q^2)\right\}, \\
\langle K_0^*(P_2)|\bar{s}\sigma_{\mu\nu}q^\nu\gamma_5 b|\overline{B}(P_B)\rangle &= \left[(m_B^2 - m_{K_0^*}^2)q_\mu - q^2 P_\mu\right]\frac{F_T(q^2)}{m_B + m_{K_0^*}},
\end{aligned}
\tag{4}
$$

while the parametrization of the $B \to K_J^*(J \geqslant 1)$ form factors is as follows [10, 17]

$$\langle K_J^*(P_2, \epsilon)|\bar{s}\gamma^\mu b|\overline{B}(P_B)\rangle = -\frac{2V(q^2)}{m_B + m_{K_J^*}}\epsilon^{\mu\nu\rho\sigma}\epsilon_{J\nu}^* P_{B\rho}P_{2\sigma},$$

$$\langle K_J^*(P_2, \epsilon)|\bar{s}\gamma^\mu \gamma_5 b|\overline{B}(P_B)\rangle = 2im_{K_J^*}A_0(q^2)\frac{\epsilon_J^* \cdot q}{q^2}q^\mu + i(m_B + m_{K_J^*})A_1(q^2)\left[\epsilon_{J\mu}^* - \frac{\epsilon_J^* \cdot q}{q^2}q^\mu\right]$$
$$-iA_2(q^2)\frac{\epsilon_J^* \cdot q}{m_B + m_{K^*}}\left[P^\mu - \frac{m_B^2 - m_{K_J^*}^2}{q^2}q^\mu\right],$$

$$\langle K_J^*(P_2, \epsilon)|\bar{s}\sigma^{\mu\nu}q_\nu b|\overline{B}(P_B)\rangle = -2iT_1(q^2)\epsilon^{\mu\nu\rho\sigma}\epsilon_{J\nu}^* P_{B\rho}P_{2\sigma},$$

$$\langle K_J^*(P_2, \epsilon)|\bar{s}\sigma^{\mu\nu}\gamma_5 q_\nu b|\overline{B}(P_B)\rangle = T_2(q^2)\left[(m_B^2 - m_{K_J^*}^2)\epsilon_{J\mu}^* - \epsilon_J^* \cdot q P^\mu\right] + T_3(q^2)\epsilon_J^* \cdot q\left[q^\mu - \frac{q^2}{m_B^2 - m_{K_J^*}^2}P^\mu\right],$$

which is in general analogous to the $B \to K^*$ ones. Here $q = P_B - P_2$, and $P = P_B + P_2$. We have the relation $2m_{K^*}A_0(0) = (m_B + m_{K_J^*})A_1(0) - (m_B - m_{K_J^*})A_2(0)$ in order to smear the pole at $q^2 = 0$. The polarization vector in the above equations is constructed by the J-rank polarization tensor

$$\epsilon_{J\mu}(h) = \frac{1}{m_B^{J-1}}\epsilon_{\mu\nu_1\nu_2...\nu_{J-1}}(h)P_B^{\nu_1}P_B^{\nu_2}...P_B^{\nu_{J-1}}, \tag{5}$$

with $h = 0, \pm 1$ being the helicity. Using the expression for $\epsilon_{\mu\nu_1\nu_2...\nu_{J-1}}(h)$ which is a product of the polarization vectors with the Clebsch-Gordan coefficients, we simplify the above equation as $\epsilon_{J\mu}(h) \sim (|\vec{p}_{K_J^*}|/m_{K_J^*})^{J-1}\tilde{\epsilon}_{J\mu}$, with $\tilde{\epsilon}_{J\mu}(0) = \alpha_L^J\epsilon_\mu(0)$ and $\tilde{\epsilon}_{J\mu}(\pm 1) = \beta_T^J\epsilon_\mu(\pm 1)$ and $|\vec{p}_{K_J^*}| \sim E_{K_J^*}$ in the large recoil region. α_L^J and β_T^J are products of the Clebsch-Gordan coefficients

$$\alpha_L^J = C_{1,0;J-1,0}^{J,0}C_{1,0;J-2,0}^{J-1,0}...C_{1,0;1,0}^{2,0},$$
$$\beta_T^J = C_{1,1;J-1,0}^{J,1}C_{1,0;J-2,0}^{J-1,0}...C_{1,0;1,0}^{2,0}. \tag{6}$$

The $B \to K_J^*$ form factors are nonperturbative in nature and the application of QCD theory to them mostly resorts to the Lattice QCD simulations, which is quite limited at this stage. The crucial input we use in this work is the observation that, in the heavy quark $m_b \to \infty$ and the large energy $E \to \infty$ limit, interactions of the heavy and light systems can be expanded in small ratios Λ_{QCD}/E and Λ_{QCD}/m_B. At the leading power, the large energy symmetry is obtained and such symmetry to a large extent simplifies the heavy-to-light transition [18, 19]. As a concrete application, the current $\bar{s}\Gamma b$ in QCD can be matched onto the current $\bar{s}_n\Gamma b_v$ constructed in terms of the fields in the effective theory. Here v denotes the velocity of the heavy meson and n is a light-like vector along the K_J^* moving direction. This procedure constrains the independent Lorentz structures and reduces the seven independent

TABLE IV: $B \to K_2^*$ form factors at $q^2 = 0$ in the ISGW2 model [21] (using the updated inputs [22]), the covariant light-front quark model [22, 23] and the light-cone QCD sum rules [17] and perturbative QCD approach [7].

	ISGW2 [22]	CLFQM [22, 23]	LCSR [17]	LEET+BSW [10]	PQCD [7]
$V^{BK_2^*}$	0.38	0.29	0.16 ± 0.02	0.21 ± 0.03	$0.21^{+0.06}_{-0.05}$
$A_0^{BK_2^*}$	0.27	0.23	0.25 ± 0.04	0.15 ± 0.02	$0.18^{+0.05}_{-0.04}$
$A_1^{BK_2^*}$	0.24	0.22	0.14 ± 0.02	0.14 ± 0.02	$0.13^{+0.04}_{-0.03}$
$A_2^{BK_2^*}$	0.22	0.21	0.05 ± 0.02	0.14 ± 0.02	$0.08^{+0.03}_{-0.02}$
$T_1^{BK_2^*}$		0.28	0.14 ± 0.02	0.16 ± 0.02	$0.17^{+0.05}_{-0.04}$
$T_3^{BK_2^*}$		-0.25	$0.01^{+0.02}_{-0.01}$	0.10 ± 0.02	$0.14^{+0.05}_{-0.03}$

hadronic form factors for each $B \to K_J^*$ ($J \geq 1$) type to two universal functions $\xi_\perp$ and $\xi_\parallel$. Explicitly, we have

$$A_0^{K_J^*}(q^2)\left(\frac{|\vec{p}_{K_J^*}|}{m_{K_J^*}}\right)^{J-1} \equiv A_0^{K_J^*,\text{eff}} \simeq (1 - \frac{m_{K_J^*}^2}{m_B E})\xi_\parallel^{K_J^*}(q^2) + \frac{m_{K_J^*}}{m_B}\xi_\perp^{K_J^*}(q^2),$$

$$A_1^{K_J^*}(q^2)\left(\frac{|\vec{p}_{K_J^*}|}{m_{K_J^*}}\right)^{J-1} \equiv A_1^{K_J^*,\text{eff}} \simeq \frac{2E}{m_B + m_{K_J^*}}\xi_\perp^{K_J^*}(q^2),$$

$$A_2^{K_J^*}(q^2)\left(\frac{|\vec{p}_{K_J^*}|}{m_{K_J^*}}\right)^{J-1} \equiv A_2^{K_J^*,\text{eff}} \simeq (1 + \frac{m_{K_J^*}}{m_B})[\xi_\perp^{K_J^*}(q^2) - \frac{m_{K_J^*}}{E}\xi_\parallel^{K_J^*}(q^2)],$$

$$V^{K_J^*}(q^2)\left(\frac{|\vec{p}_{K_J^*}|}{m_{K_J^*}}\right)^{J-1} \equiv V^{K_J^*,\text{eff}} \simeq (1 + \frac{m_{K_J^*}}{m_B})\xi_\perp^{K_J^*}(q^2),$$

$$T_1^{K_J^*}(q^2)\left(\frac{|\vec{p}_{K_J^*}|}{m_{K_J^*}}\right)^{J-1} \equiv T_1^{K_J^*,\text{eff}} \simeq \xi_\perp^{K_J^*}(q^2),$$

$$T_2^{K_J^*}(q^2)\left(\frac{|\vec{p}_{K_J^*}|}{m_{K_J^*}}\right)^{J-1} \equiv T_2^{K_J^*,\text{eff}} \simeq (1 - \frac{q^2}{m_B^2 - m_{K_J^*}^2})\xi_\perp^{K_J^*}(q^2),$$

$$T_3^{K_J^*}(q^2)\left(\frac{|\vec{p}_{K_J^*}|}{m_{K_J^*}}\right)^{J-1} \equiv T_3^{K_J^*,\text{eff}} \simeq \xi_\perp^{K_J^*}(q^2) - (1 - \frac{m_{K_J^*}^2}{m_B^2})\frac{m_{K_J^*}}{E}\xi_\parallel^{K_J^*}(q^2). \tag{7}$$

For the sake of simplicity we will use the latter set of form factors but as in the case of C_9 and C_7, we drop the superscript "eff" as well. In the case of B to scalar meson transition, the large energy limit gives

$$\frac{m_B}{m_B + m_{K_0^*}}F_T(q^2) = F_1(q^2) = \frac{m_B}{2E}F_0(q^2) = \xi^{K_0^*}(q^2). \tag{8}$$

The results for $\xi_\parallel^{K_J^*}$ and $\xi_\perp^{K_J^*}$ derived from the Bauer-Stech-Wirbel (BSW) model [20] in Ref. [10] will be used in this work and we collect these results in Tab. III. For the $B \to K_0^*$ transition, it is plausible to employ $\xi^{B \to K_0^*} = \xi_\parallel^{B \to K_2^*}$ since both K_0^* and K_2^* are p-wave states.

Several remarks on the form factors are given in order.

- Due to the lack of Lattice QCD simulations, the calculation of $B \to K_J^*$ form factors rely on different phenomenological models. In Tab. IV, as an example we show the results for the $B \to K_2^*$ form factors at $q^2 = 0$ in the ISGW2 model [21] (using the updated inputs [22]), the covariant light-front quark model [22, 23] and the light-cone QCD sum rules [17] and perturbative QCD approach [7] (using the light meson's light-cone distribution amplitudes [24]). From this table we can see the LEET+BSW results used here are close to the ones in the light-cone sum rules (except for T_3) and the perturbative QCD approach.

- The large energy effective theory [18, 19] has neglected the interaction between the soft sector and collinear sector and it is refined by the soft-collinear effective theory [25–29], in which at leading power in $1/m_b$ a form factor takes the generic expression

$$F_i(q^2) = C_i \xi(q^2) + C_i' \int d\tau \Xi_a(\tau, q^2). \tag{9}$$

Here C_i and C_i' are the short-distance Wilson coefficients obtained by integrating out degrees of freedom with virtuality of $\mathcal{O}(m_b^2)$. ξ is one of the above universal functions entering the large-recoil symmetries. $\Xi_a(\tau, q^2)$ is a symmetry breaking function, which can be factorized into a convolution of light-cone distribution amplitudes with the jet function. The detailed expressions of the $B \to K_J^*$ form factors (with the subscript "eff") have a similar form with the $B \to V$ transition, for instance, as Eqs.(21, 22) in Ref. [30] and in particular, two relations for form factors remain

$$\frac{m_B}{m_B + m_{K_J^*}} V^{K_J^*} = \frac{m_B + m_{K_J^*}}{2E} A_1^{K_J^*}, \quad T_1^{K_J^*} = \frac{m_B}{2E} T_2^{K_J^*}. \tag{10}$$

Again, the function ξ can only be calculated in some nonperturbative QCD methods. The calculation in light-cone sum rules in conjunction with the soft-collinear effective theory indicates that the ξ dominates in $B \to \pi$ transition while the Ξ_a gives corrections at the order of $5\% - 10\%$ [31] [1]. One may expect a similar size for Ξ_a in $B \to K_J^*$ transition which will be one of the main sources of uncertainties.

- It is noteworthy to point out that there are ambiguities in the internal structures of K_0^*, thus large discrepancies on form factors can be found in the literature. For instance, using two different assignments of K_0^*, namely p-wave states without or with one unit of radial excitation, we have calculated the B to scalar meson form factors in perturbative QCD approach [34] and the results can differ up to a factor of 3 [35]. We propose that the $SU(3)$-symmetry related processes can be used to pin down the uncertainties. Channels of this type include the semi-leptonic $B \to a_0(1450)l\bar{\nu}$, $B_s \to K_0^* l\bar{\nu}$ decays and the exclusive channels $\bar{B}^0 \to a_0^+(1450)D_s^-/D^-$, $B^- \to a_0^0(1450)D_s^-$, $\bar{B}_s \to K_0^{*+}D^-$. Semileptonic decays provide the information of form factors in the full kinematics region through the differential decay width distribution. The above exclusive processes are color-favored and free of annihilation diagrams; therefore the factorization method works phenomenologically well for them. In the factorization context, the decay amplitudes, taking $\bar{B}^0 \to D_s^- a_0^+(1450)$ as an example, are written as

$$\mathcal{A}(\bar{B}^0 \to D_s^- a_0^+) = \frac{iG_F}{\sqrt{2}} i V_{cs}^* V_{ub} a_1 f_{D_s}(m_B^2 - m_{D_s}^2) F_0^{B \to a_0}(m_{D_s}^2), \tag{11}$$

where $a_1 \sim 1$ being the Wilson coefficients and f_{D_s} denoting the decay constant of the D_s meson. In particular, most of the inputs will be canceled if the ratio

$$r = \frac{\Gamma(\bar{B}^0 \to D_s^- a_0^+)}{\Gamma(\bar{B}^0 \to D_s^- \pi^+)} \simeq \frac{[F_0^{B \to a_0}(m_{D_s}^2)]^2}{[F_0^{B \to \pi}(m_{D_s}^2)]^2}$$

is considered. The decay $\bar{B}^0 \to D_s^- \pi^+$ has a quite large branching ratio $\mathcal{B} = (2.4 \pm 0.4) \times 10^{-5}$ [14]. The measurement of $\bar{B}^0 \to D_s^- a_0^+$ in the future will consequently determine the $F_0^{B \to a_0}$ and also $F_0^{B \to K_0^*}$ up to $SU(3)$ symmetry breaking effects. Replacing D_s^- by D_s^{*-}, one can extract the form factor $F_1^{B \to a_0/K_0^*}$ from the relevant data in future.

---

[1] A direct fit of the hadronic $B \to \pi\pi$ decay data results in a large $\Xi_a^{B \to \pi}$ [32], while a numerically small $\Xi_a^{B \to \rho}$ seems to be favored by the $B \to \rho\rho$ data [33].

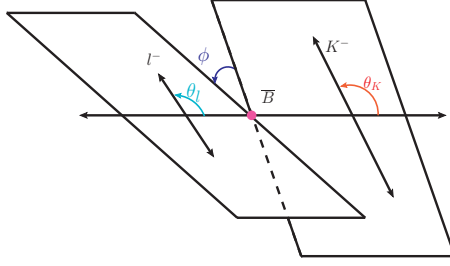FIG. 1: Kinematics in $\overline{B} \to \overline{K}_J^*(\to K^-\pi^+)l^+l^-$. K_J^* moves along the z axis in the B rest frame. $\theta_K(\theta_l)$ is defined in K_J^* (lepton pair) rest frame as the angle between z-axis and the flight direction of K^- (μ^-), respectively. The azimuth angle ϕ is the angle between the K_J^* decay and lepton pair planes.

III. DIFFERENTIAL DECAY DISTRIBUTIONS AND FORWARD-BACKWARD ASYMMETRIES

The convention on the kinematics in $B \to K_J^*(\to K\pi)l^+l^-$ is illustrated in Fig. 1. The moving direction of K_J^* in the B rest frame is chosen as the z axis. The polar angle θ_K (θ_l) is defined as the angle between the flight direction of K^- (μ^-) and the z axis in the K_J^* (lepton pair) rest frame. ϕ is the angle defined by the decay planes of K_J^* and the lepton pair.

$B \to K_J^*(\to K\pi)l^+l^-$ is a quasi four-body decay process and proceeds via three steps: B meson first decays into a nearly onshell strange meson plus a pair of leptons; the K_J^* meson propagates followed by its strong decay into the $K\pi$ state. The decay amplitudes of $B \to (K^-\pi^+)l^+l^-$ are obtained by sandwiching Eq. (1) between the initial and final states, in which the spinor product $[\bar{s}b]$ by hadronic matrix element will be replaced by hadronic form factors. The operator realization of this picture is

$$\langle l^+l^-|[\bar{l}l]|0\rangle\langle K\pi|[\bar{s}b]|\overline{B}^0\rangle \; \simeq \; \langle l^+l^-|[\bar{l}l]|0\rangle \int d^4p_{K_J^*} \frac{\langle K\pi|K_J^*\rangle\langle K_J^*|[\bar{s}b]|\overline{B}^0\rangle}{p_{K_J^*}^2 - m_{K_J^*}^2 + im_{K_J^*}\Gamma_{K_J^*}}, \tag{12}$$

with $p_{K_J^*}^2 = m_{K\pi}^2$. In appendix A, we will compute the required quantities in the three steps with the use of helicity amplitudes. Combining the individual pieces, we obtain the angular distributions

$$\begin{aligned}
\frac{d^4\Gamma}{dm_{K\pi}^2 dq^2 d\cos\theta_K d\cos\theta_l d\phi} \;=\; &\Big[I_1^c + 2I_1^s + (I_2^c + 2I_2^s)\cos(2\theta_l) + 2I_3\sin^2\theta_l\cos(2\phi) + 2\sqrt{2}I_4\sin(2\theta_l)\cos\phi \\
&+ 2\sqrt{2}I_5\sin(\theta_l)\cos\phi + 2I_6\cos\theta_l + 2\sqrt{2}I_7\sin(\theta_l)\sin\phi \\
&+ 2\sqrt{2}I_8\sin(2\theta_l)\sin\phi + 2I_9\sin^2\theta_l\sin(2\phi)\Big],
\end{aligned} \tag{13}$$

with the angular coefficients

$$
\begin{aligned}
I_1^c &= (|A_{L0}|^2 + |A_{R0}|^2) + 8\frac{m_l^2}{q^2}\text{Re}[A_{L0}A_{R0}^*] + 4\frac{m_l^2}{q^2}|A_t|^2, \\
I_1^s &= \frac{3}{4}[|A_{L\perp}|^2 + |A_{L||}|^2 + |A_{R\perp}|^2 + |A_{R||}|^2]\left(1 - \frac{4m_l^2}{3q^2}\right) + \frac{4m_l^2}{q^2}\text{Re}[A_{L\perp}A_{R\perp}^* + A_{L||}A_{R||}^*], \\
I_2^c &= -\beta_l^2(|A_{L0}|^2 + |A_{R0}|^2), \\
I_2^s &= \frac{1}{4}\beta_l^2(|A_{L\perp}|^2 + |A_{L||}|^2 + |A_{R\perp}|^2 + |A_{R||}|^2), \\
I_3 &= \frac{1}{2}\beta_l^2(|A_{L\perp}|^2 - |A_{L||}|^2 + |A_{R\perp}|^2 - |A_{R||}|^2), \\
I_4 &= \frac{1}{\sqrt{2}}\beta_l^2[\text{Re}(A_{L0}A_{L||}^*) + \text{Re}(A_{R0}A_{R||}^*)], \qquad I_5 = \sqrt{2}\beta_l[\text{Re}(A_{L0}A_{L\perp}^*) - \text{Re}(A_{R0}A_{R\perp}^*)], \\
I_6 &= 2\beta_l[\text{Re}(A_{L||}A_{L\perp}^*) - \text{Re}(A_{R||}A_{R\perp}^*)], \qquad I_7 = \sqrt{2}\beta_l[\text{Im}(A_{L0}A_{L||}^*) - \text{Im}(A_{R0}A_{R||}^*)], \\
I_8 &= \frac{1}{\sqrt{2}}\beta_l^2[\text{Im}(A_{L0}A_{L\perp}^*) + \text{Im}(A_{R0}A_{R\perp}^*)], \qquad I_9 = \beta_l^2[\text{Im}(A_{L||}A_{L\perp}^*) + \text{Im}(A_{R||}A_{R\perp}^*)].
\end{aligned}
\tag{14}
$$

The lepton mass correction factor is $\beta_l = \sqrt{1 - 4m_l^2/q^2}$. The functions $A_{L/Ri}$ are defined by

$$
A_{L/R0/t} = \sum_{J=0,1,2\ldots} \sqrt{N_{K_J^*}}Y_J^0(\theta,0)\mathcal{M}_B(K_J^*, L/R, 0/t)\frac{i}{m_{K\pi}^2 - m_{K_J^*}^2 + im_{K_J^*}\Gamma_{K_J^*}}\sqrt{\frac{m_{K_J^*}\Gamma_{K_J^*\to K\pi}}{\pi}},
$$

$$
A_{L/R||/\perp} = \sum_{J=0,1,2\ldots} \sqrt{N_{K_J^*}}Y_J^{-1}(\theta,0)\mathcal{M}_B(K_J^*, L/R, ||/\perp)\frac{i}{m_{K\pi}^2 - m_{K_J^*}^2 + im_{K_J^*}\Gamma_{K_J^*}}\sqrt{\frac{m_{K_J^*}\Gamma_{K_J^*\to K\pi}}{\pi}},
$$

with $N_{K_J^*} = \frac{\sqrt{\lambda}q^2\beta_l}{256\pi^3 m_B^3}$. $\mathcal{M}_B$ is the decay amplitudes of $B \to K_J^* V$ to be given in the appendix. In the narrow-width limit, the integration over the $K\pi$ invariant mass will be conducted as

$$
\int dm_{K\pi}^2 \frac{m_{K_J^*}\Gamma_{K_J^*}}{\pi}\frac{1}{(m_{K\pi}^2 - m_{K_J^*}^2)^2 + m_{K_J^*}^2\Gamma_{K_J^*}^2} = 1.
\tag{15}
$$

Integrating out the angles θ_l, θ_K and ϕ, we obtain the dilepton mass spectrum

$$
\begin{aligned}
\frac{d^2\Gamma_L}{dq^2 dm_{K\pi}^2} &= \frac{2}{3}\int_{-1}^{1} 2\pi d\cos\theta_K\,(3I_1^c - I_2^c), \\
\frac{d^2\Gamma_T}{dq^2 dm_{K\pi}^2} &= \frac{2}{3}\int_{-1}^{1} 2\pi d\cos\theta_K\,(6I_1^s - 2I_2^s), \\
\frac{d^2\Gamma}{dq^2 dm_{K\pi}^2} &= \frac{d^2\Gamma_L}{dq^2 dm_{K\pi}^2} + \frac{d^2\Gamma_T}{dq^2 dm_{K\pi}^2},
\end{aligned}
\tag{16}
$$

and its expression in the massless limit

$$
\frac{d^2\Gamma_i}{dq^2 dm_{K\pi}^2} = \frac{8}{3}\int_{-1}^{1} 2\pi d\cos\theta_K(|A_{Li}|^2 + |A_{Ri}|^2),
\tag{17}
$$

with $i = 0, \pm 1$ or $i = 0, \perp, ||$.

The differential FBA in this process is defined by

$$
\frac{d^2 A_{FB}}{dq^2 dm_{K\pi}^2} = \left[\int_0^1 - \int_{-1}^0\right]d\cos\theta_l \frac{d^3\Gamma}{dq^2 d\cos\theta_l dm_{K\pi}^2} = \frac{2}{3}\int_{-1}^{1} 2\pi\cos\theta_K 3I_6,
\tag{18}
$$

while the normalized differential FBA is given by

$$
\frac{\overline{d^2 A_{FB}}}{dq^2 dm_{K\pi}^2} = \frac{\frac{d^2 A_{FB}}{dq^2 dm_{K\pi}^2}}{\frac{d^2\Gamma}{dq^2 dm_{K\pi}^2}} = \frac{\int_{-1}^{1} d\cos\theta_K 3I_6}{\int_{-1}^{1} d\cos\theta_K[3I_1^c + 6I_1^s - I_2^c - 2I_2^s]}.
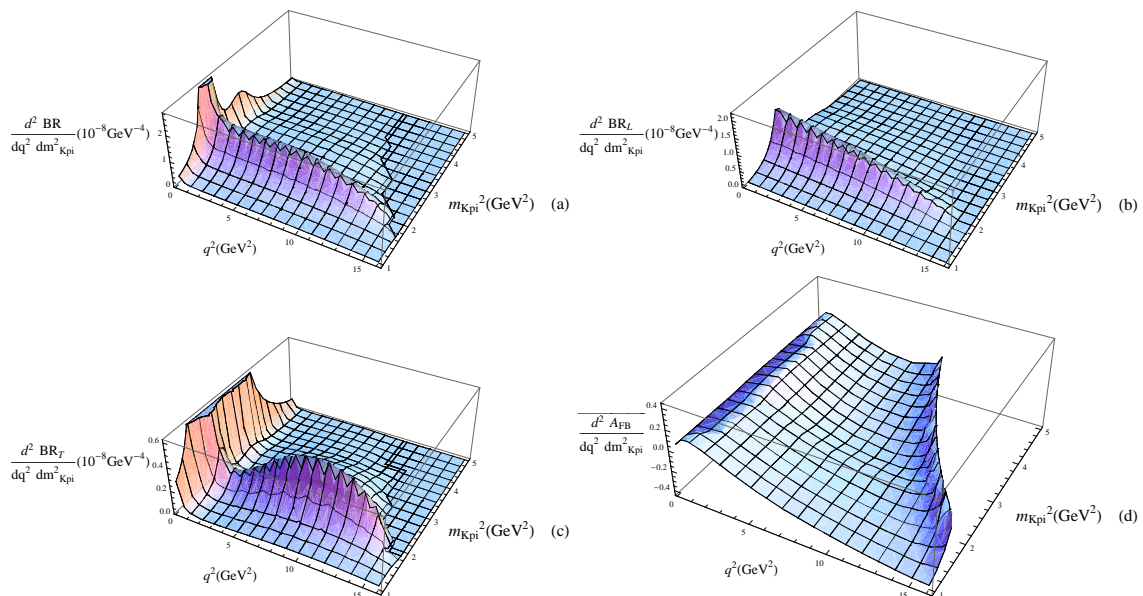\tag{19}
$$

FIG. 2: Differential branching ratios $\frac{d^2 BR_i}{dq^2 dm_{K\pi}^2}$, with i denoting the total (a), longitudinal (b) and transverse polarizations (c), and the normalized FBA $\frac{\overline{d^2 A_{FB}}}{dq^2 dm_{K\pi}^2}$ (d) for $\bar{B}^0 \to K^- \pi^+ \mu^+ \mu^-$ in the mass region $1 \text{GeV}^2 < m_{K\pi}^2 < 5 \text{GeV}^2$

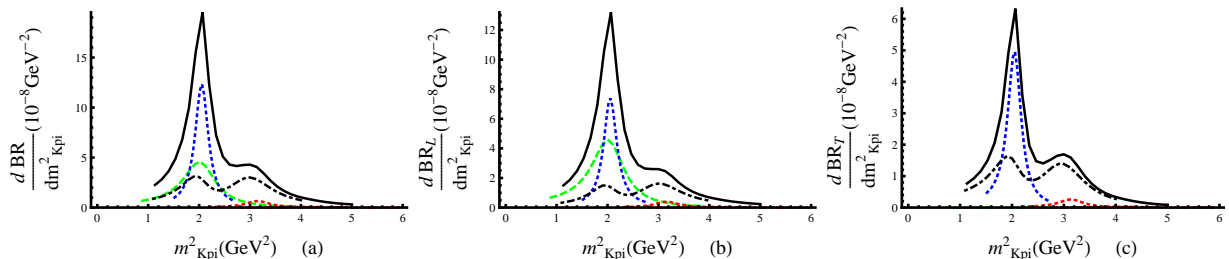FIG. 3: Differential branching ratios $\frac{dBR_i}{dm_{K\pi}^2}(\overline{B}^0 \to K^- \pi^+ \mu^+ \mu^-)$ integrated over the kinematics region $q^2 > 4m_l^2$. The black (solid) curve denotes the total contribution, while individual terms are given by the green (dashed) line for $K_0^*(1430)$, blue dotted line for $K_2^*(1430)$, the black (dot-dashed) line for $K^*(1680)$ and $K^*(1410)$ with the interference incorporated, and the red (dotted) curve with a very small magnitude for $K_3^*(1780)$. The contribution from $K_4^*(2045)$ is negligibly small.

IV. NUMERICAL RESULTS AND DISCUSSIONS

Before presenting the numerical results, we start with an estimate of the contributions from different mesons. It is noticed that larger the J is the smaller is the contribution. (1) The K_J^* with a larger spin is heavier and thus the phase space is smaller. (2) The Clebsch-Gordan coefficient products α_L^J and β_T^J decrease with the increase of J. (3) The $B \to K_J^*$ form factors suppress the heavier K_J^* further. Moreover, the tiny branching ratios of $K^*(1410)$ and $K_4^*(2045)$ into $K^- \pi^+$ result in very smaller effects. As a consequence we find that the $K_4^*(2045)$ is negligibly small.

We plot the differential branching ratios $\frac{d^2 BR_i}{dq^2 dm_{K\pi}^2}$ (in units of 10^{-8}GeV^{-4}), with the subscript i denoting the total, longitudinal and transverse polarizations) and the normalized FBA $\frac{\overline{d^2 A_{FB}}}{dq^2 dm_{K\pi}^2}$ for $\bar{B}^0 \to K^- \pi^+ \mu^+ \mu^-$ in Fig. 2. By integrating the differential distributions over q^2, we obtain their dependence on $m_{K\pi}^2$. Fig. 3 shows the differential branching ratios $\frac{dBR_i}{dm_{K\pi}^2}(\overline{B}^0 \to K^- \pi^+ \mu^+ \mu^-)$ (in units of 10^{-8}GeV^{-2}) integrated over the kinematics region $4m_l^2 <$
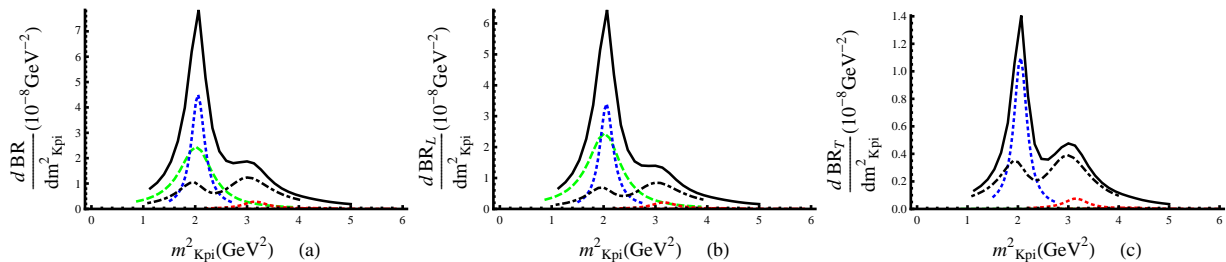
FIG. 4: Same as Fig. 3, but integrated over $1\text{GeV}^2 < q^2 < 6\text{GeV}^2$

$q^2 < (m_B - m_{K\pi})^2$, while Fig. 4 gives the results under the integration over $1\text{GeV}^2 < q^2 < 6\text{GeV}^2$. In these figures, the black (solid) curve denotes the total contribution, while individual terms are given by the green (dashed) line for $K_0^*(1430)$, blue dotted line for $K_2^*(1430)$, the black (dot-dashed) line for $K^*(1680)$ and $K^*(1410)$ with the interference incorporated, and the red (dotted) curve with a very small magnitude for $K_3^*(1780)$. The contribution from $K_4^*(2045)$ is negligibly small. From these figures, we can see that for $m_{K\pi}^2 = 2\text{GeV}^2$, the K_2^* dominates; while at $m_{K\pi}^2 \simeq 3\text{GeV}^2$, the $B \to K^*(1680)$ contribution is the largest, especially in the transverse polarization.

Now let us analyze the zero crossing point s_0 of FBAs satisfying $\frac{d^2 A_{FB}}{dq^2 dm_{K\pi}^2}|_{q^2=s_0} = 0$ and governed by the equation

$$\text{Re}[C_9]A_1(s_0)V(s_0) + C_{7L}\frac{m_b(m_B + m_{K_J^*})}{s_0}A_1(s_0)T_1(s_0) + C_{7L}\frac{m_b(m_B - m_{K_J^*})}{s_0}T_2(s_0)V(s_0) = 0. \qquad (20)$$

Substituting the relations from the large energy limit into the above equation, we find that the dependence on the form factors cancels completely and more explicitly Eq. (20) gives

$$s_0 = (3.1 \pm 0.1)\text{GeV}^2, \qquad (21)$$

where the uncertainties are caused by $m_{K_J^*}^2/m_B^2$ corrections in the form factor relations in Eq. (7). As we have discussed in Sec. II, the interaction of collinear and soft sectors brings in symmetry breaking effects. After the inclusion of them, only two relations among form factors remain as in Eq. (10). Define the ratio

$$\mathcal{R}^{K_J^*}(q^2) \equiv \frac{m_B + m_{K_J^*}}{m_B}\frac{T_1^{K_J^*}(q^2)}{V^{K_J^*}(q^2)}, \qquad (22)$$

we find that Eq. (20) becomes

$$\text{Re}[C_9] + 2\frac{m_b m_B}{s_0}C_{7L}\mathcal{R}^{K_J^*}(s_0) = 0. \qquad (23)$$

The analaysis in Ref. [30] indicates that the ratio $\mathcal{R}$ can deviate from 1 by 10% in the $B \to V$ transition (see Eq.(124) of [30]). Using the PQCD [7] and LCSR [17] results for the $B \to K_2$ form factors, we have

$$\mathcal{R}_{\text{PQCD}}^{K_2} \sim 1.03, \quad \mathcal{R}_{\text{LCSR}}^{K_2} \sim 1.11, \qquad (24)$$

where the q^2-dependence is negligible since form factors T_1 and V are found to have similar q^2-distribution in both model calculations. Suppose that the $\mathcal{R}^{K_J^*}$ deviates from 1 by 10%, the s_0 is also shifted by roughly 10%, namely 0.3 GeV^2.

Our analysis of the $m_{K\pi}$ dependence can be generalized to similar channels such as $\bar{B}^0 \to J/\psi K_J^* \to (\mu^+\mu^-)(K^-\pi^+)$ and $B_s \to f_J(\to K^+K^-)l^+l^-$. For the former processes, however, apart from the $B \to K_J^*$ form factors, it is likely that the effective Wilson coefficients a_2 depends on the spin of K_J^* as well (for a recent discussion see Ref. [36]).

Although the relative strengths among K_J^* may be modified, the structure of the dependence on $m_{K\pi}^2$ is expected to be similar. For the latter, uncertainties are presumably smaller, as a recent measurement of $B_s \to J/\psi K^+ K^-$ clearly shows the peak at $f_2'(1525)$ [37].

V. CONCLUSION

In summary, we have analyzed the resonant contributions in the process $\overline{B}^0 \to K^- \pi^+ \mu^+ \mu^-$ with the $K^- \pi^+$ invariant mass square $m_{K\pi}^2 \in [1,5]\mathrm{GeV}^2$. Width effects of the strange mesons involved in this range, $K^*(1410), K_0^*(1430), K_2^*(1430), K^*(1680), K_3^*(1780)$ and $K_4^*(2045)$, are incorporated. In terms of the helicity amplitudes, we derive a compact form for the full angular distributions, through which the branching ratios, forward-backward asymmetries and polarizations are attained. To pin down the uncertainties in the form factors, we suggest the measurements of a set of SU(3)-related processes which are useful. Using the form factors from the large energy limit, we derive the dependence of the branching fractions on $m_{K\pi}$, and we point out that the K_2^* and $K^*(1680)$ contributions can be separated from the rest, in particular, in the transverse polarizations. The generalization into $\bar{B} \to J/\psi K_J^*(\to K^- \pi^+)$ and $B_s \to f_J(\to K^+ K^-)l^+ l^-$ is also discussed briefly.

Acknowledgements

Appendix A: Helicity amplitudes

The differential distributions are divided into several individual pieces and each of them can be expressed in terms of the helicity amplitudes which are Lorentz invariant.

- B decays into K_J^*

  The spin-0 K_0^* in the final state has only one polarization state and the longitudinal amplitudes are

  $$
  \begin{aligned}
  i\mathcal{M}_B(K_0^*, L/R, 0) &= N_1 i \left[(C_9 \mp C_{10}) \frac{\sqrt{\lambda}}{\sqrt{q^2}} F_1(q^2) + 2(C_{7L} - C_{7R}) \frac{\sqrt{\lambda} m_b}{\sqrt{q^2}(m_B + m_{K_0^*})} F_T(q^2) \right], \\
  i\mathcal{M}_B(K_0^*, L/R, t) &= N_1 i \left[(C_9 \mp C_{10}) \frac{m_B^2 - m_{K_0^*}^2}{\sqrt{q^2}} F_0(q^2) \right],
  \end{aligned}
  \tag{A1}
  $$

  with $N_1 = \frac{iG_F}{4\sqrt{2}} \frac{\alpha_{\mathrm{em}}}{\pi} V_{tb} V_{ts}^*$. The function λ is related to the magnitude of the K_J^* momentum in B meson rest frame: $\lambda \equiv \lambda(m_B^2, m_{K_J^*}^2, q^2) = 2m_B|\vec{p}_{K_J^*}|$, and $\lambda(a^2, b^2, c^2) = (a^2 - b^2 - c^2)^2 - 4b^2c^2$. Here the script t denotes the time-like component of a virtual vector/axial-vector meson decays into a lepton pair. In the case of strange

mesons with spin $J \geq 1$, the $K^- \pi^+$ system can be either longitudinally or transversely polarized:

$$
i\mathcal{M}_B(K_J^*, L, 0) = \frac{\alpha_L^J N_1 i}{2 m_{K_J^*} \sqrt{q^2}} \left[(C_9 - C_{10})[(m_B^2 - m_{K_J^*}^2 - q^2)(m_B + m_{K_J^*})A_1 - \frac{\lambda}{m_B + m_{K_J^*}}A_2] \right.
$$
$$
\left. + 2m_b(C_{7L} - C_{7R})[(m_B^2 + 3m_{K_J^*}^2 - q^2)T_2 - \frac{\lambda}{m_B^2 - m_{K_J^*}^2}T_3] \right],
$$

$$
i\mathcal{M}_B(K_J^*, L, \pm) = \beta_T^J N_1 i \left[(C_9 - C_{10})[(m_B + m_{K_J^*})A_1 \mp \frac{\sqrt{\lambda}}{m_B + m_{K_J^*}}V] \right.
$$
$$
\left. - \frac{2m_b(C_{7L} + C_{7R})}{q^2}(\pm \sqrt{\lambda}T_1) + \frac{2m_b(C_{7L} - C_{7R})}{q^2}(m_B^2 - m_{K_J^*}^2)T_2 \right], \tag{A2}
$$

$$
i\mathcal{M}_B(K_J^*, L, t) = \alpha_L^J i N_1 (C_9 - C_{10}) \frac{\sqrt{\lambda}}{\sqrt{q^2}} A_0. \tag{A3}
$$

For the sake of convenience, we define

$$
i\mathcal{M}_B(K^*, L, \perp/\|) = \frac{1}{\sqrt{2}}[i\mathcal{M}_B(K^*, L, +) \mp i\mathcal{M}_B(K^*, L, -)],
$$

$$
i\mathcal{M}_B(K^*, L, \perp) = -i\beta_T^J \sqrt{2} N_1 \left[(C_9 - C_{10})\frac{\sqrt{\lambda}V}{m_B + m_{K_J^*}} + \frac{2m_b(C_{7L} + C_{7R})}{q^2}\sqrt{\lambda}T_1 \right],
$$

$$
i\mathcal{M}_B(K^*, L, \|) = i\beta_T^J \sqrt{2} N_1 \left[(C_9 - C_{10})(m_B + m_{K_J^*})A_1 + \frac{2m_b(C_{7L} - C_{7R})}{q^2}(m_B^2 - m_{K_J^*}^2)T_2 \right]. \tag{A4}
$$

The right-handed decay amplitudes are defined in a similar way

$$
A_{Ri} = A_{Li}|_{C_{10} \to -C_{10}}. \tag{A5}
$$

The combination of the time-like decay amplitude is used in the differential distribution

$$
i\mathcal{M}_B(K_0^*, t) = i\mathcal{M}_B(K_0^*, R, t) - i\mathcal{M}_B(K_0^*, L, t) = 2\alpha_L^J i C_{10} N_1 \frac{m_B^2 - m_{K_0^*}^2}{\sqrt{q^2}} F_0(q^2), \tag{A6}
$$

$$
i\mathcal{M}_B(K_J^*, t) = i\mathcal{M}_B(K_J^*, R, t) - i\mathcal{M}_B(K_J^*, L, t) = 2\alpha_L^J i N_1 C_{10} \frac{\sqrt{\lambda}}{\sqrt{q^2}} A_0(q^2). \tag{A7}
$$

- Nonzero leptonic amplitudes are given as follows

$$
\mathcal{M}_{L,R}(\lambda_l, \lambda_{\bar{l}}, \lambda_V) = T_{\lambda_l, \lambda_{\bar{l}}}^{L,R} D_{\lambda_V, \lambda_l - \lambda_{\bar{l}}}^{1*}(\phi, \pi - \theta_l, 0),
$$

$$
\mathcal{M}_L(\frac{1}{2}, \frac{1}{2}, t) = -\mathcal{M}_L(\frac{-1}{2}, \frac{-1}{2}, t) = -\mathcal{M}_R(\frac{1}{2}, \frac{1}{2}, t) = \mathcal{M}_R(\frac{-1}{2}, \frac{-1}{2}, t) = -2m_l. \tag{A8}
$$

with $q_{\pm} = \sqrt{q^2} \pm \sqrt{q^2 - 4m_l^2}$. The reduced matrix elements are given as

$$
T_{\frac{1}{2}\frac{1}{2}}^L = T_{\frac{-1}{2}\frac{-1}{2}}^L = T_{\frac{1}{2}\frac{1}{2}}^R = T_{\frac{-1}{2}\frac{-1}{2}}^R = -2m_l,
$$

$$
T_{\frac{1}{2}\frac{-1}{2}}^L = T_{\frac{-1}{2}\frac{1}{2}}^R = \sqrt{2}q_-, \quad T_{\frac{-1}{2}\frac{1}{2}}^L = T_{\frac{1}{2}\frac{-1}{2}}^R = -\sqrt{2}q_+. \tag{A9}
$$

- The propagation of K_J^* is parameterized by a Breit-Wigner formula while the $K_J^* \to K\pi$ decay is described by the spherical harmonic functions: $Y_J^i(\theta_K, 0)$, with $i = 0$ for K_0^* and $i = 0, \pm 1$ for K_J^*. It should be pointed out that the dependence of the coupling between a virtual K_J^* and the $K\pi$ state on $m_{K\pi}^2$ is neglected. Since there is no singularity in the coupling, it can be expanded in terms of $m_{K\pi}^2 - m_{K_J^*}^2$ around the resonance region, which

is also guaranteed by the Breit-Wigner propagation. For definiteness, we list the explicit forms of the spherical harmonic functions used in this work

$$Y_0^0(\theta_K, \phi) = \frac{1}{\sqrt{4\pi}}, \quad Y_1^0(\theta_K, \phi) = \sqrt{\frac{3}{4\pi}} \cos \theta_K, \quad Y_1^{\pm 1}(\theta_K, \phi) = \mp \sqrt{\frac{3}{8\pi}} \sin \theta_K,$$

$$Y_2^0(\theta_K, \phi) = \sqrt{\frac{5}{16\pi}} (3 \cos^2 \theta_K - 1), \quad Y_2^{\pm 1}(\theta_K, \phi) = \mp \sqrt{\frac{15}{32\pi}} \sin(2\theta_K),$$

$$Y_3^0(\theta_K, \phi) = \sqrt{\frac{7}{16\pi}} (5 \cos^3 \theta_K - 3 \cos \theta_K), \quad Y_3^{\pm 1}(\theta_K, \phi) = \mp \sqrt{\frac{21}{64\pi}} \sin \theta_K (5 \cos^2 \theta_K - 1),$$

$$Y_4^0(\theta_K, \phi) = \frac{3}{16\sqrt{\pi}} (35 \cos^4 \theta_K - 30 \cos^2 \theta_K + 3), \quad Y_4^{\pm 1}(\theta_K, \phi) = \mp \frac{3\sqrt{5}}{8\sqrt{\pi}} \sin \theta_K (7 \cos^3 \theta_K - 3 \cos \theta_K). \quad (A10)$$

[1] B. Aubert *et al.* [BABAR Collaboration], Phys. Rev. Lett. **102**, 091803 (2009) [arXiv:0807.4119 [hep-ex]].

[2] J. T. Wei *et al.* [BELLE Collaboration], Phys. Rev. Lett. **103**, 171801 (2009) [arXiv:0904.0770 [hep-ex]].

[3] T. Aaltonen *et al.* [CDF Collaboration], Phys. Rev. D **79**, 011104 (2009) [arXiv:0804.3908 [hep-ex]].

[4] The LHCb Collaboration, LHCb-CONF-2011-038.

[5] C. Bobeth, G. Hiller and D. van Dyk, JHEP **1107**, 067 (2011) [arXiv:1105.0376 [hep-ph]].
See also A. Ali, P. Ball, L. T. Handoko *et al.*, Phys. Rev. **D61**, 074024 (2000). [hep-ph/9910221]; F. Kruger and J. Matias, Phys. Rev. D **71**, 094009 (2005) [arXiv:hep-ph/0502060]; U. Egede, T. Hurth, J. Matias, M. Ramon, W. Reece, JHEP **0811**, 032 (2008) [arXiv:0807.2589 [hep-ph]]; W. Altmannshofer, *et al.*, JHEP **0901**, 019 (2009) [arXiv:0811.1214 [hep-ph]]; and many references therein.

[6] R. -H. Li, C. -D. Lu, W. Wang, Phys. Rev. **D83**, 034034 (2011) [arXiv:1012.2129 [hep-ph]].

[7] W. Wang, Phys. Rev. D **83**, 014008 (2011) [arXiv:1008.5326 [hep-ph]].

[8] S. Rai Choudhury, A. S. Cornell, G. C. Joshi, B. H. J. McKellar, Phys. Rev. **D74**, 054031 (2006). [hep-ph/0607289].

[9] S. R. Choudhury, A. S. Cornell, N. Gaur, Phys. Rev. **D81**, 094018 (2010). [arXiv:0911.4783 [hep-ph]].

[10] H. Hatanaka and K. C. Yang, Phys. Rev. D **79**, 114008 (2009) [arXiv:0903.1917 [hep-ph]]; Eur. Phys. J. C **67**, 149 (2010) [arXiv:0907.1496 [hep-ph]].

[11] N. Katirci, K. Azizi, JHEP **1107**, 043 (2011) [arXiv:1105.3636 [hep-ph]].

[12] M. Junaid, M. J. Aslam, [arXiv:1103.3934 [hep-ph]].

[13] T. M. Aliev, M. Savci, [arXiv:1109.2738 [hep-ph]].

[14] K. Nakamura *et al.* [Particle Data Group], J. Phys. G **37**, 075021 (2010).

[15] G. Buchalla, A. J. Buras and M. E. Lautenbacher, Rev. Mod. Phys. **68**, 1125 (1996) [arXiv:hep-ph/9512380].

[16] A. J. Buras and M. Munz, Phys. Rev. D **52**, 186 (1995) [arXiv:hep-ph/9501281].

[17] K. -C. Yang, Phys. Lett. **B695**, 444-448 (2011) [arXiv:1010.2944 [hep-ph]].

[18] M. J. Dugan and B. Grinstein, Phys. Lett. B **255**, 583 (1991).

[19] J. Charles, A. Le Yaouanc, L. Oliver, O. Pene and J. C. Raynal, Phys. Rev. D **60**, 014001 (1999) [hep-ph/9812358].

[20] M. Wirbel, B. Stech, M. Bauer, Z. Phys. **C29**, 637 (1985).

[21] D. Scora and N. Isgur, Phys. Rev. D **52**, 2783 (1995) [hep-ph/9503486].

[22] H. -Y. Cheng and K. -C. Yang, Phys. Rev. D **83**, 034001 (2011) [arXiv:1010.3309 [hep-ph]].

[23] H. -Y. Cheng and C. -K. Chua, Phys. Rev. D **81**, 114006 (2010) [Erratum-ibid. D **82**, 059904 (2010)] [arXiv:0909.4627 [hep-ph]].

[24] H. Y. Cheng, Y. Koike and K. C. Yang, Phys. Rev. D **82**, 054019 (2010) [arXiv:1007.3541 [hep-ph]].

[25] C. W. Bauer, S. Fleming, D. Pirjol, I. W. Stewart, Phys. Rev. **D63**, 114020 (2001) [hep-ph/0011336].

[26] C. W. Bauer, S. Fleming and M. E. Luke, Phys. Rev. D **63**, 014006 (2000) [hep-ph/0005275].

[27] C. W. Bauer, D. Pirjol, I. W. Stewart, Phys. Rev. Lett. **87**, 201806 (2001) [hep-ph/0107002].

[28] C. W. Bauer, D. Pirjol and I. W. Stewart, Phys. Rev. D **65**, 054022 (2002) [hep-ph/0109045].

[29] C. W. Bauer, D. Pirjol and I. W. Stewart, Phys. Rev. D **67**, 071502 (2003) [hep-ph/0211069].

[30] M. Beneke and D. Yang, Nucl. Phys. B **736**, 34 (2006) [hep-ph/0508250].

[31] F. De Fazio, T. Feldmann and T. Hurth, Nucl. Phys. B **733**, 1 (2006) [Erratum-ibid. B **800**, 405 (2008)] [hep-ph/0504088].

[32] C. W. Bauer, D. Pirjol, I. Z. Rothstein and I. W. Stewart, Phys. Rev. D **70**, 054015 (2004) [hep-ph/0401188].

[33] A. Jain, I. Z. Rothstein and I. W. Stewart, arXiv:0706.3399 [hep-ph].

[34] Y. Y. Keum, H. n. Li and A. I. Sanda, Phys. Lett. B **504**, 6 (2001) [arXiv:hep-ph/0004004]; Phys. Rev. D **63**, 054008 (2001) [arXiv:hep-ph/0004173]; C. D. Lu, K. Ukai and M. Z. Yang, Phys. Rev. D **63**, 074009 (2001) [arXiv:hep-ph/0004213]; C. D. Lu, and M. Z. Yang, Eur. Phys. J. C **23**, 275-287 (2002) [arXiv:hep-ph/0011238].

[35] R. -H. Li, C. -D. Lu, W. Wang, X. -X. Wang, Phys. Rev. **D79**, 014013 (2009); W. Wang, Y. -L. Shen, Y. Li, C. -D. Lu, Phys. Rev. **D74**, 114010 (2006); Y. -L. Shen, W. Wang, J. Zhu, C. -D. Lu, Eur. Phys. J. **C50**, 877-887 (2007); C. s. Kim, Y. Li and W. Wang, Phys. Rev. D **81**, 074014 (2010).

[36] P. Colangelo, F. De Fazio, W. Wang, Phys. Rev. **D81**, 074001 (2010); Phys. Rev. **D83**, 094027 (2011); W. Wang, AIP Conf. Proc. **1317**, 304 (2011) [arXiv:1010.1924 [hep-ph]].

[37] R. Aaij *et al.* [LHCb Collaboration], arXiv:1112.4695 [hep-ex] and also LHCb-CONF-2011-035.